THE JOURNAL OF PHYSICAL CHEMISTRY

Freie Universität Berlin

Subscriber access provided by UB + Fachbibliothek Chemie | (FU-Bibliothekssystem)

Article

6-Mercaptopurine Self-Assembled Monolayers on Gold (001)-hex: Revealing the Fate of Gold Adatoms

Pilar Carro, Kathrin Müller, Flavia Lobo Maza, Carolina Vericat, Ulrich Starke, Klaus Kern, Roberto C. Salvarezza, and Doris Grumelli

J. Phys. Chem. C, **Just Accepted Manuscript** • DOI: 10.1021/acs.jpcc.7b02732 • Publication Date (Web): 05 Apr 2017

ACS Publications

The Journal of Physical Chemistry C is published by the American Chemical Society. 1155 Sixteenth Street N.W., Washington, DC 20036

6-Mercaptopurine Self-Assembled Monolayers on Gold (001)-hex: Revealing the Fate of Gold Adatoms

Pilar Carro[1], Kathrin Müller[2], Flavia Lobo Maza[3], Carolina Vericat[3], Ulrich Starke[2], Klaus Kern[2,4], Roberto C. Salvarezza[3] and Doris Grumelli[3*]

[1] *Área de Química Física, Departamento de Química, Facultad de Ciencias, Universidad de La Laguna, Instituto de Materiales y Nanotecnología, Avda. Francisco Sánchez, s/n 38200-La Laguna, Tenerife, Spain*

[2] *Max Planck Institute for Solid State Research, Heisenbergstrasse 1, D-70569 Stuttgart, Germany*

[3] *Instituto de Investigaciones Fisicoquímicas Teóricas y Aplicadas (INIFTA), Facultad de Ciencias Exactas, Universidad Nacional de La Plata - CONICET- Sucursal 4 Casilla de Correo 16, (1900) La Plata, Argentina*

4 Institut de Physique, Ecole Polytechnique Fédéerale de Lausanne, 1015 Lausanne, Switzerland

[*]Corresponding author: Doris Grumelli

email : doris@inifta.unlp.edu.ar

Abstract

Thiol molecules adsorbed on gold have long ago become a model system for molecular self-assembly on metal substrates. In most cases the strong molecule-gold interaction is able to restructure the substrate, resulting in vacancy islands and steps. Today it is widely accepted that gold adatoms produced by this process form stable thiol-adatom complexes, usually termed "staples" (RS-Au_{ad}-SR or RS-Au_{ad}-SR-Au_{ad}-SR), which are the basic units of the self-assembled monolayers. Here we report on a different scenario for 6-mercaptopurine (6MP), a heterocyclic aromatic thiol, namely its adsorption on the Au(001)-(5×20) reconstructed surface. Our results show that 6MP lifts the reconstruction upon adsorption, thus ejecting a large excess of gold adatoms. Surprisingly, 6MP molecules prefer to arrange in highly ordered adatom-free domains in the bridging configuration, while the ejected adatoms form gold islands. Our investigation reveals that the formation of thiol-gold adatom complexes is not always a thermodynamically favored process but rather depends on the nature of the thiol molecule.

Introduction

One of the key structural components in self-assembled monolayers (SAMs) of thiolates (RS) on Au surfaces are gold adatoms (Au_{ad}), that form different thiol-adatom complexes commonly called staples (either RS-Au_{ad}-SR or RS-Au_{ad}-SR-Au_{ad}-SR species)[1-2] which have been identified on thiol-protected Au nanoclusters (AuNC)[3] and also on the surface of well-ordered thiolate SAMs on Au(111).[4] In the former case, AuNC grow in the presence of Au(III) ions and thiolates, so that the staples could be formed as a product of the synthesis or by attack of the thiolates to the growing clusters resulting in gold atom removal from the surface.[2, 5] This last mechanism is evident during the self-assembly of alkanethiols on the Au(111) surface, where they induce the formation of either serrated steps or vacancy islands at terraces as a result of adatom ejection leading to staples formation. From the stoichiometry of the gold complexes, 0.16 Au_{ad} ML are needed for the typical saturation coverage of thiols $\theta = 0.33$ ML.[6] In this case there is also a small contribution of 0.05 of Au_{ad} arising from the lifting of the Au(111)-(22×√3) reconstruction (the "herringbone" reconstruction) which is induced by thiol adsorption. It is now broadly accepted that staples are a general and thermodynamically favored binding motif of alkanethiolates on Au(111), a fact that has been confirmed by DFT calculations.[1]

In contrast, a general feature for the adsorption of small-sized aromatic thiols (with one or two aromatic rings) on Au(111) is that they lift the herringbone reconstruction and generate gold steps, but fail to produce vacancy islands, i.e. they are unable to extract Au atoms from terraces. In fact, rather than vacancy islands aromatic thiols induce the formation of small islands which have been assigned either to gold structures and/or to molecular aggregates.[7-8] The failure of small aromatic thiols to form staple moieties has been explained considering their lower coverage and adsorption energy compared to alkanethiols (they do not compensate the energy cost to extract the Au atoms from the terraces).[9] Similar arguments

have been used to explain the absence of staples when 6-mercaptopurine (6MP, Figure 1), a small aromatic thiol of relevance for the treatment of some leukemias and autoimmune conditions because of its role as purine antagonist[10], is adsorbed on the Au(111)[7] and Au(001)-(1×1) surfaces.[11] However, there is also another possible reason for this behavior: a low chemical affinity of the aromatic molecules to the Au adatoms, a fact that could also explain the formation of Au islands rather than vacancy Au islands.

In this manuscript, we have placed 6MP molecules in a completely different scenario in order to test the molecule-Au_{ad} reactivity on the substrate surface. 6MP was adsorbed on the Au(001)-(5×20) (hereafter denoted as Au(001)-(hex)) surface, which exhibits a hexagonal surface reconstruction with a higher density of Au atoms in the first layer (0.25 ML of additional Au atoms).[12] If the adsorption of molecules is able to lift the hex surface reconstruction then they would be in contact with a large amount of ejected Au adatoms (θ_{ad} =0.25) whose fate would account for the affinity of the aromatic molecules to form the staples units. Our results from low-energy electron diffraction (LEED), scanning tunneling microscopy (STM), x-ray photoelectron spectroscopy (XPS), electrochemical measurements and density functional theory (DFT) calculations show that 6MP molecules indeed lift the hex reconstruction and chemisorb through a S-Au bond. However, they prefer to organize in well-ordered staple-free lattices in a bridging configuration with gold adatoms forming small and irregular islands, i.e. this aromatic molecule is not prone to form staple moieties.

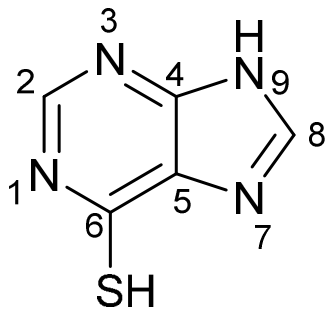

Figure1. Chemical structure of the 6-mercaptopurine (6MP) molecule

Experimental Methods

Sample preparation

Au(001) single-crystal substrates (MaTeck) were cleaned by repeated cycles of sputtering with Ar^+ ions and annealing at 825 K under ultra-high vacuum (UHV) leading to the Au(001)-(hex) surface reconstruction,[12] which has been confirmed by LEED and STM. This surface is characterized by stripes 1.45 nm wide separated by 0.07 nm deep channels. SAMs of 6MP (Aldrich, 98%) were prepared by immersion of the Au(001)-hex surfaces in 100 μM 6MP ethanolic solutions (BASF 99%) for 30 min. Then the samples were removed from the solution, rinsed with ethanol and dried under N_2 before they were reintroduced into UHV.

STM imaging

Samples were imaged in a home-made UHV STM operating at room temperature. W tips were used with 100-600 mV tunneling voltages and 100-350 pA tunneling currents. The STM was calibrated in x, y and z directions using the stripes of the well-known Au(001)-hex surface reconstruction. WsXM software was used for image analysis. [13]

Electrochemical experiments

A home-built sample transfer system between UHV and electrochemical environment was used. After preparation or characterization the samples were brought to the transfer chamber and argon atmosphere (5.0 purity, p = 1 bar) was established.

Cyclic voltammetry was made with an Autolab PGSTAT30 potentiostat and a three-electrode conventional electrochemical cell. A large area Pt coil was used as counter electrode and a silver/silver chloride (3M KCl) electrode was employed as reference electrode (RE). All the potentials in the text are referred to that RE. Aqueous 0.1 M NaOH solutions were prepared by using NaOH pellets (Sigma-Aldrich; 99.99 % trace metals basis) and ultrapure water with 18.2 MΩcm resistivity (Millipore Products, Bedford).

Thiol reductive electrodesorption curves were performed at room temperature by scanning the potential from -0.3 V to -1.4 V at 0.05 Vs^{-1} in the 0.1 M NaOH solution. In each case the charge density (q) involved in the reductive desorption peak was obtained by integration of the peak area. The geometrical area of the single crystal electrode (0.196 cm^2) was used to calculate the current densities. This figure was taken as an indication of the surface coverage of the thiol SAM.

XPS and LEED measurements

XPS and LEED measurements were performed in a separate UHV system. The freshly prepared 6MP SAMs were transferred into the UHV system. Photoemission experiments for 6MP SAMs were carried out in a commercial KRATOS AXIS ULTRA system with a monochromatized Al Kα source with a base pressure in the lower 10^{-10} mbar range. The binding energy (BE) scales for the SAMs on Au surfaces were calibrated by setting the Au $4f_{7/2}$ BE to 84.0 eV with respect to the Fermi level. High-resolution S 2p, N 1s, C 1s and Au 4f spectra were acquired with an analyzer pass energy of 20 eV.

Analysis of the XPS data was performed with CasaXPS v 2.3.84 software. Shirley type backgrounds were subtracted from the spectra before the fitting procedure and peaks that are a combination of Lorenzian and Gaussian functions were employed for all regions. In the case of the S 2p signal, the spin-orbit doublet separation was fixed at 1.18 eV and an area ratio of 2:1 was used. The atomic concentrations were calculated by using calculated photoemission cross-sections according to Yeh and Lindau.[14]

LEED data were acquired in the same UHV system using a commercial SPECS ErLEED 1000-A. LEEDPAT software[15] was used to simulate the obtained LEED patterns. The LEED of the clean Au(001)-hex surface was obtained after cleaning the sample in the same UHV system and transferring it into the LEED chamber without breaking the vacuum.

Computational Methods

Density functional calculations were performed with the periodic plane-wave basis set code VASP 5.2.12.[16-17] The scheme of non-local functional proposed by Dion et al,[18] vdW-DF, and the optimized Becke88 exchange functional optB88-vdW[19] were used to take into account van der Waals (vdW) interactions. The projector augmented plane wave (PAW) method was used to represent the atomic cores using the PBE potential.[20] The electronic wave functions were expanded in a plane-wave basis set with a 420 eV cutoff energy. Optimal grids of Monkhorst-Pack[21] k-points 2×9×1 were used for numerical integration in the reciprocal space of the (6×√2) unit cell used to simulate the (3√2×√2)R45° surface structure described in the experimental results section. Because 6MP adsorption lifts the hex-reconstruction we have used a Au(001)-(1×1) substrate represented by five atomic layers and a vacuum of ~17 Å that separates two successive slabs in our calculation. Surface relaxation is allowed in the three uppermost Au layers of the slab, as well as the atomic coordinates of the adsorbed species, were allowed to relax without further constraints. The atomic positions were relaxed until the force on the unconstrained atoms was < 0.03 eVÅ^{-1}. The adsorbates were placed just on one side of the slab and all calculations include a dipole correction. The adsorbed 6MP species, taken as thiyl radicals[22] were optimized in an asymmetric box of 20 Å × 20 Å × 40 Å. The calculated Au lattice constant is 4.16 Å, which compares reasonably well with the experimental value (4.078 Å).[23] The average binding energy per adsorbed 6MP species on Au(001)-(1×1) surfaces, E_b, is defined in Eq. [1]:

$$E_b = \frac{1}{N_{thiol}}\left[E^{thiol/Au} - E^{Au} - N_{thiol}E^{thiol}\right] \qquad [1]$$

where, $E^{thiol/Au}$, E^{Au} and E^{thiol} stand for the total energy of the adsorbate-substrate system, the total energy of the Au slab, and the energy of the 6MP radical, respectively, whereas N_{thiol} is the number of 6MP radicals in the surface unit cell. A negative number indicates that adsorption is exothermic with respect to the separate clean surface and 6MP radical. The

Gibbs free energy of adsorption of each surface structure (γ) was approximated through the total energy from DFT calculations by using equation [2]:

$$\gamma = \frac{N_{thiol}E_b + E_{rec}}{A} \qquad [2]$$

where E_{rec} is the reconstruction energy per unit cell defined by,

$$E_{rec} = E^{R}_{Au(100)} - E^{U}_{Au(100)} - n_{ad}E^{Au}_{bulk}$$

where $E^{R}_{Au(100)}$ and $E^{U}_{Au(100)}$ correspond to the energy of reconstructed Au(001) surface and unreconstructed Au(001) surface per unit cell, respectively; E^{Au}_{bulk} is the total energy of a bulk Au atom, n_{ad} is the number of Au adatoms in the surface unit cell and A is the unit cell area. Considering that we are concerned with free energy differences, it is reasonable to assume that the contributions coming from the configurational entropy, the vibrations and the work term pV, can be neglected. DFT calculations make systematic (but unknown) errors relative to the true solution of the Schrödinger equation because of the approximate nature of the exchange-correlation functional. However if two DFT calculations compare chemically similar states, then the systematic errors in these two calculations are also similar. In other words, relative energies can be calculated accurately. In this sense, we can therefore expect a good level of accuracy in the adsorption energy.

Results and Discussion

The LEED pattern of the clean Au(001) shown in Figure 2a is consistent with that already reported for the well-known (5×20) hex reconstruction.[24] Clean surfaces were then used for the self-assembly of the 6MP molecules by immersion in the 6MP ethanolic solution for 30 min.

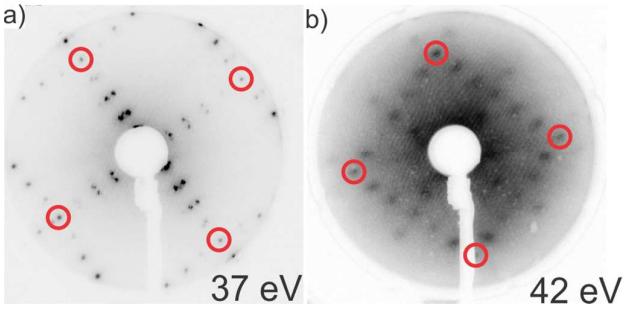

Figure 2. LEED patterns for (a) the clean Au(001)-hex surface and (b) the same substrate after a 30 min immersion in 6MP solution. Note that the LEED patterns are rotated with respect to each other due to different mounting orientations of the sample. The (1,0) main spots are marked by red circles for easier comparison.

After immersion of the Au(001)-hex substrate into the 6MP ethanolic solution a LEED pattern showing a $(3\sqrt{2}\times\sqrt{2})R45°$ reconstruction, commensurate with the Au(001) substrate, was obtained (Figure 2b). This gives a rectangular unit cell with unit cell parameters of 1.22×0.41 nm^2. The unit cell is rotated by 45° with respect to the <110> direction of the Au surface. Furthermore, one can notice that none of the spots in the LEED pattern coincides with those of the hex surface reconstruction (Figure 2a), evidencing that it has been lifted during the 6MP self-assembly. In contrast, immersion of the reconstructed substrate in pure ethanol for a similar time period does not affect the hex surface, i.e. ethanol adsorption is not able to lift the reconstruction (data not shown).

STM gives local information on how 6MP molecules organize on the Au substrate. The images show that most of the surface exhibits a large number of irregular islands 2-6 nm in size (Figure 3a) and height $h \approx 0.2$ nm (Figure 3b). This value indicates that they are mostly Au islands resulting from the lifting of the hex reconstruction. The islands contain also an internal corrugation with $h \approx 0.03$-0.05 nm (Figure 3b) suggesting that they are covered by 6MP molecules (see arrows in Figure 3c). The small corrugation value is consistent with molecular features dominated by electronic rather than topographic effects. The islands coexist with ordered molecular domains formed by stripes (Figure 3a) that also exhibit $h \approx$

0.05 nm across them (Figure 3b). Note also that the stripes intersect steps at 45°, while two adjacent striped domains intersect at 90° (Figure 3c).

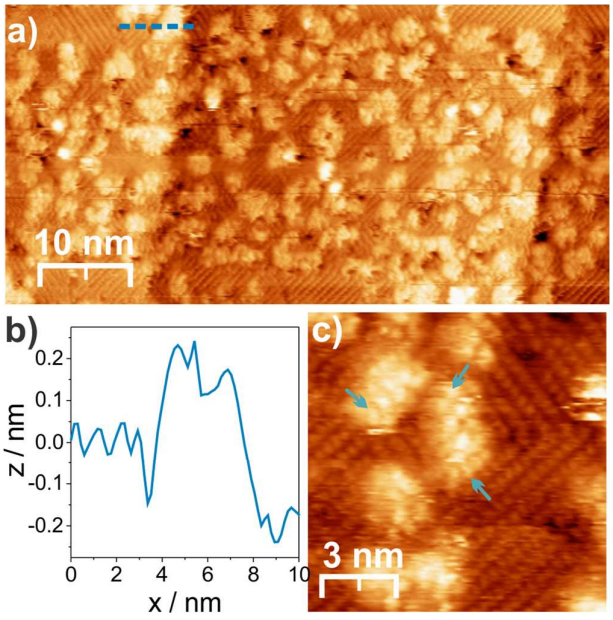

Figure 3 (a) Large scale STM image of 6MP on Au(001)-(hex) showing stripes and irregular Au islands (b) cross-section along the blue dashed line in (a) showing the height of the islands, molecular features (left side and top of the island) and a step (right side) .(c) High resolution STM image of 6MP on Au(001)-(hex) showing disordered molecules adsorbed on the islands (blue arrows).

The diffuse edges and irregular shape of these islands (Figure 3a,c) contrast the well-defined square or rectangular Au islands formed by electrochemical lifting of the hex reconstruction in the absence of aromatic thiol molecules.[12] We recall that the lifting induced either by adsorption of molecules or by changing the electrochemical potential results in the expelling of Au_{ad} in an equivalent amount to θ_{ad} = 0.25 ML[25] which either nucleate and grow into islands or reach step edges. It seems that the diffusion path of the Au_{ad} is much smaller for the adsorption induced lifting presumably because the molecular lattice blocks the movement of the Au adatoms, thus leading to smaller and more irregular islands that are also covered by 6MP molecules (see arrows in Figure 3c). The estimation of the island coverage is difficult due to their irregular shape with disordered molecules at the boundaries, and also probably by convolution of the tip with the small islands, but a rough estimation yields about $\theta_{isl} \approx 0.3$,

slightly larger than that expected considering that they are formed from the reconstruction (θ_{ad} = 0.25). This situation is completely different when 6MP adsorption takes place directly on the Au(100)-(1×1) surface, where the molecules are not in contact with a large population of free Au adatoms. In this case the shape and size of the islands formed by electrochemical lifting remain unchanged after 6MP adsorption, i.e. the absorption process itself is not strong enough to mobilize a large amount of Au_{ad}.[11]

The STM image in Figure 4 was obtained in a particular region where there are practically no Au_{ad} islands. Although areas like this are an exception we can still consider it to determine the molecular structure of the ordered domains coexisting with the islands. The image shows Au(001) terraces covered by rotated domains which were formed either by stripes where it is difficult to resolve individual molecules (red arrow in Figure 4a, phase A), or by stripes where individual molecules can be clearly distinguished (green arrow in Figure 4a, phase B). Note that there are no vacancy islands (depth=0.24 nm) on the terraces; instead we observe pinholes as dark holes corresponding to molecular vacancies (blue arrows in Figure 4a) with depth < 0.24 nm.

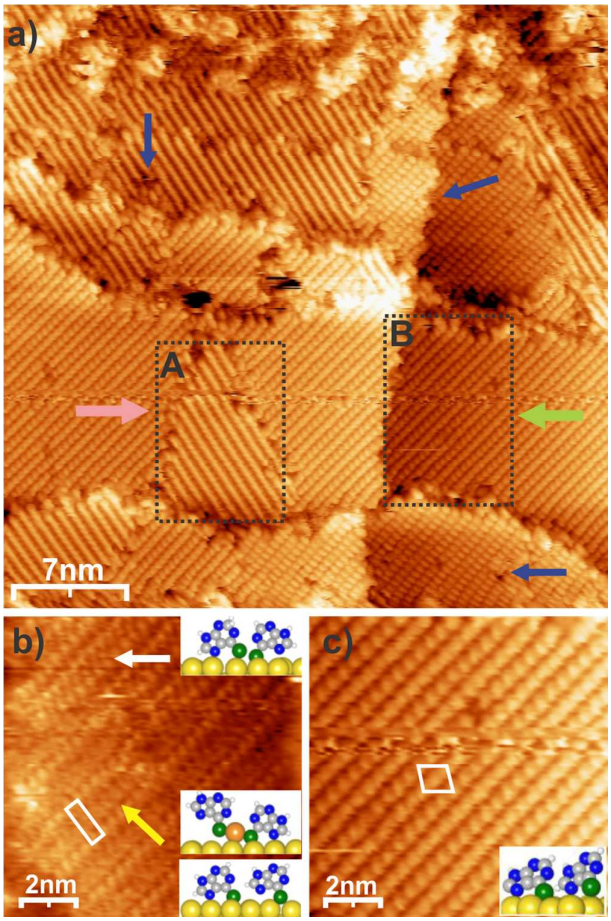

Figure 4. STM images of the 6MP-covered Au(001)-(hex) surface. (a) STM image (background subtraction) showing flat terraces and 6MP stripped phases: A domains (red arrow) and B domains (green arrow). Steps and pinholes are also indicated (blue arrows). (b) High resolution STM image of type A domain. The head-to-tail (white arrow) and head-to-head (yellow arrow) configurations, unit cell (white) and molecular arrangements from DFT models are also indicated. (c) High resolution STM image of type B domain. The unit cell (white) and the molecular arrangement from DFT model (taken from Ref 11) are indicated. Key: Au atoms (yellow), Au_{ad} (orange), S atoms (green), C atoms (grey), N atoms (blue), H atoms (white).

Figure 4b shows the molecular structure of type A domains. At the upper left side of the image (white arrow) we can see bright rows separated by 0.65±0.03 nm. In the remaining part of Figure 4b one can see that one of the bright rows is absent so that they are separated by ≈ 1.3±0.05 nm (Figure 4b). Inside the rows we can detect individual spots separated by 0.42±0.03 nm. Both structures can be related to the $(3\sqrt{2}\times\sqrt{2})R45°$ superstructure detected by LEED. The 0.65 nm dimension is close to the size of the 6MP molecule that has an elongated

shape while the ≈ 0.4 nm distance inside the rows results from optimization of the π-π interactions between adjacent aromatic rings. We propose head-to-tail (largely the most abundant) and head-to-head arrangements to explain the smaller (0.65 nm) and larger (1.3 nm) separation between bright rows shown in Figure 4b. In fact, while the head-to-tail configuration was observed for this molecule on Au(100)-(1×1)[11] the head-to-head configuration has been frequently observed for different alkanethiols arranged parallel to the substrate.[26-28]. The larger size of the bright spots when the molecules are separated by ≈ 1.3 nm suggests that they result from the convolution of the two adjacent S atoms, one from each molecule which, according to the literature, could form a disulfide bond [26] or a staple unit by trapping one Au_{ad}[29] (see schemes in Figure 4b-c). Therefore, both molecular arrangements exhibit the same surface coverage θ = 0.33 (see also Figure SI-1a).

On the other hand, type B domains consist of rows of bright spots that closely resemble the elongated shape of the 6MP molecule. The spots in neighboring rows are shifted forming quasi-rhomboidal structures with 0.5±0.03 nm and 0.7±0.03 nm intra and inter row distances, respectively (Figure 4c). These structures can be described as a (3×√10) lattice with θ = 0.22 (see Figure SI-1b) as already reported for 6MP on Au(001)-(1×1)[11], a fact that confirms the lifting of the hex reconstruction to form the (1×1) surface due to 6MP adsorption.

High resolution XPS has been used to explore the different chemical species present in the 6MP covered Au(001)-(hex) surface. The S 2p spectrum (Figure SI-2a) reveals the presence of chemisorbed thiols[6] without evidence of atomic sulfur or oxidized sulfur species, in agreement with previous data for this molecule on the Au(111)[7] and Au(001)-(1×1) surfaces.[11] More important, the absence of the component corresponding to physisorbed thiols (at ≈ 163.5 eV) indicates that the disordered islands observed in the STM images are not aggregates of unbounded molecules. Also, the N 1s and C 1s XPS spectra (Figure SI-2b,c) are similar to those reported for 6MP on the Au(001)-(1×1)[11] and Au(111)[7] and

consistent with the adsorption of intact dehydrogenated 6MP molecules, which are bound to the Au surface as thiolates.

We have performed reductive desorption curves in order to estimate the surface coverage of 6MP on the Au(001)-hex surface. The curves show a main sharp peak located at a peak potential E_p = -0.81 V (Figure SI-3) which appears at the same potentials as those found for 6MP on the Au(100)-(1×1)[11], which is another evidence for the lifting of the hex reconstruction upon 6MP adsorption. The charge density (q) involved in the peak for the Au(100) surface is q =47±7 μC cm^{-2} from which a thiol coverage θ = 0.25 is obtained.[30-31] In the present case it should be an average of the dense A and diluted B domains, as well as of the molecules adsorbed on the disordered Au island regions.

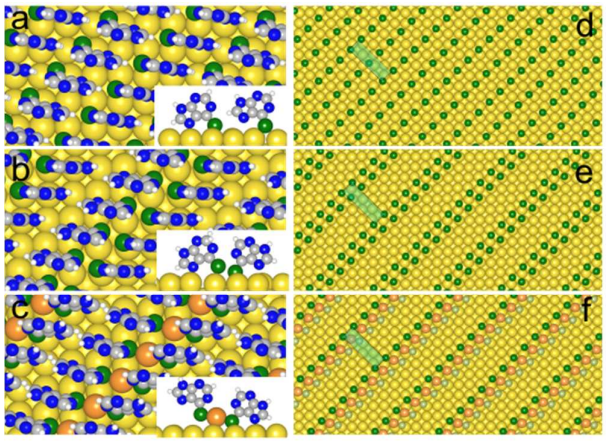

Figure 5. Optimized surface models on Au(001)-(1×1). (a, d): head-to-tail, (b, e): head-to-head, (c, f): head-Au_{ad}-head. (a-c) Top views. Insets: side views. Key: Au atoms (yellow), Au_{ad} (orange), S atoms (green), C atoms (grey), N atoms (blue), H atoms (white). (d-f) Positions of the S heads (green) and Au adatoms (orange) for the different models. In (f) the disconnected S atom is shown in light green. In (d-f) the unit cell is indicated in green.

DFT calculations were used to model the (3√2×√2)R45° surface structure containing two 6MP per unit cell in both head-to-tail (Figure 5 a, d) and head-to-head configurations (Figure 5b,e). In the head-to-tail configuration (Figure 5 a, d) the 6MP molecules are bonded through their respective S atom at twofold bridge sites of the Au(001) surface, following the directions [110] and $[1\bar{1}0]$ and with the aromatic rings of both molecules oriented almost in

the same direction. Besides, it can be observed that only one of the two 6MP (tilt angle 36º) is bound also on an Au atop site of the surface by the N(7) atom, while the N(7) atom of the other 6MP (tilt angle 26º) is further away from the surface. Furthermore, we have simulated the head-to-head arrangements of the $(3\sqrt{2}\times\sqrt{2})R45°$ lattice with two models whose main difference is the absence (Figure 5 b, e) or presence of Au_{ad}[29] (Figure 5c, f). In this case the adatom placed at a bridge site connects the S atoms of the two molecules, forming RS-Au_{ad}-SR units.

On the other hand, we have assigned domain B type to the more diluted $(3\times\sqrt{10})$ with θ = 0.22 that has been already proposed for 6MP molecules adsorbed on the Au(001)-(1×1) after electrochemical lifting of the hex surface.[11] The surface structure of domain B has been described by a rhomboidal $(3\times\sqrt{10})$ unit cell that consists of 6MP molecules forming rows of rectangles 0.53×0.73 nm^2 in size rotated $\approx 45°$ with respect to the substrate unit cell. Molecules are bonded through the S atoms which are placed at bridge and on top sites of the Au surface and by N(7) atoms at top sites. The tilt angle of the molecular plane with respect to the surface normal is $\alpha \approx 40º$.

Now we will focus our analysis on the thermodynamic stability (γ) of these models (see methods and Table 1- SI). The head-to-head configuration (Figure 5 b, e) exhibits the lowest stability (γ =-108.17 meVÅ^{-2}) due to its low adsorption energy (E_b), which is largely improved by introducing the Au_{ad} in the structure to form RS-Au_{ad}–SR moieties (Figure 5c and f). However, in this case we need an extra energy cost per 6MP to reconstruct the 1x1 surface and make Au_{ad} available (E_{rec}= +0.52 eV). This energy cost markedly reduces the thermodynamic stability to γ = -117.92 meVÅ^{-2}, although it is still more stable than the adatom-free head-to-head configuration. Interestingly, we note that one of the S atoms of the staple initially bonded to the Au surface was, after optimization, spontaneously disconnected from the substrate (Figure 5f). On the other hand, the head-to-tail configuration (Figure 5a

and d) exhibits the highest thermodynamic stability (γ =-128.87 meVA^{-2}) of the three models. Finally, the (3×√10) lattice exhibits a similar binding energy E_b = -3.24 eV (equation [1] and SI- Table 1) but a much lower thermodynamic stability γ =-83.3 meVA^{-2} because of its lower molecular density.

The larger thermodynamic stability of the (3√2×√2) R45° lattices than that of the (3×√10) lattice can be explained by the larger number of thiolate bonds ([equation 2]) and the optimization of intermolecular forces by π-π stacking between the aromatic rings. Therefore, during self-assembly B domains should be slowly transformed into the more stable A domains as more 6MP molecules are adsorbed. In fact, Figure SI-1 c) shows that this process is possible by simple incorporation of additional 6MP molecules to the substrate, thus demonstrating the connection between the two surface structures. However, the coexistence of different phases in thiols SAMs at room temperature is a well-known phenomenon[6] where molecules are kinetically trapped in metastable states, hindering the formation of denser phases. [29, 32]

Importantly the head-to-tail configuration (Figure 5a, d), the dominant (3√2×√2)R45° 6MP structure on Au(001)-(1×1), is inconsistent with the presence of staples because the 0.4 nm distance is too small to accommodate these moieties, and because the molecules cannot maintain a parallel orientation due the S atom hybridization. Also, for the (3×√10) lattice the position and the orientation of the two 6MP molecules with their respective aromatic ring almost parallel do not allow the formation of the RS-Au$_{ad}$-SR complex. In this case the Au$_{ad}$ should be bonded between both moieties through S-Au bonds since the S atom is sp^3 hybridized with bond angles of nearly 109.5º. [11]

Conclusions

Our results for 6MP adsorption on the Au(001)-(hex) surface reveal the low tendency of these aromatic thiol molecules to form ordered lattices containing staple moieties. The absence of

staples was also observed for this molecule on Au(111)[7] although in this case one could argue that adsorption was too weak to extract adatoms from terraces, as the lifting of the herringbone reconstruction only provides a negligible amount of adatoms (θ_{ad} = 0.05). The energy cost to extract adatoms from terraces could also explain the absence of staples when 6MP adsorption is performed directly on the Au(001)-(1×1) surface.[11] In contrast, for the Au(001)-hex surface the lifting of the reconstruction provides a large excess of Au_{ad} (θ_{ad} = 0.25) so that this argument is not valid, i.e. there are always enough Au_{ad} to form the staple moieties. However, even in this situation 6MP molecules organize to yield a bridging configuration while the ejected Au_{ad} are trapped inside the ordered lattices forming irregular Au islands. Therefore, our investigation reveals that the formation of thiol-gold adatom complexes is not always a thermodynamically favored process and depends strongly on the nature of the thiol molecule. To sum up, we present a new scenario in the surface chemistry of the thiol-gold system: a correct selection of the thiol molecule allows us to tailor the structure of the thiol-Au interface in SAMs, which opens the possibility for applications where tailor-made interfaces are relevant.

Supporting Information

Supporting information contains graphical explanation of phase transition from domain B to domain A and their units cells, XPS plots, electrochemical reductive desorption of 6MP and table containing the energetic and structural data for 6MP surface structure on Au(001)-hex obtained by DFT.

Acknowledgements

The authors acknowledge financial support from ANPCyT (PICT 2012-0836) and CONICET (PIP 0093). P.C. acknowledges MINECO (ENE2016-74889-C4-2-R, AEI-FEDER-UE). F. L.

M. acknowledges a doctoral fellowship from CONICET and a Max Planck Stipendium in Prof. Kern´s group.

References

(1) Hakkinen, H. The Gold-Sulfur Interface at the Nanoscale. *Nat. Chem.* **2012**, *4*, 443-455.
(2) Pensa, E.; Cortés, E.; Corthey, G.; Carro, P.; Vericat, C.; Fonticelli, M. H.; Benítez, G.; Rubert, A. A.; Salvarezza, R. C. The Chemistry of the Sulfur–Gold Interface: In Search of a Unified Model. *Acc. Chem. Res.* **2012**, *45*, 1183-1192.
(3) Jadzinsky, P. D.; Calero, G.; Ackerson, C. J.; Bushnell, D. A.; Kornberg, R. D. Structure of a Thiol Monolayer-Protected Gold Nanoparticle at 1.1 Å Resolution. *Science* **2007**, *318*, 430-433.
(4) Cossaro, A.; Mazzarello, R.; Rousseau, R.; Casalis, L.; Verdini, A.; Kohlmeyer, A.; Floreano, L.; Scandolo, S.; Morgante, A.; Klein, M. L., et al. X-Ray Diffraction and Computation Yield the Structure of Alkanethiols on Gold(111). *Science* **2008**, *321*, 943-946.
(5) Reimers, J. R.; Ford, M. J.; Marcuccio, S. M.; Ulstrup, J.; Hush, N. S. Competition of Van Der Waals and Chemical Forces on Gold–Sulfur Surfaces and Nanoparticles. *Nat. Rev. Chem.* **2017**, *1*, 0017.
(6) Vericat, C.; Vela, M. E.; Benitez, G.; Carro, P.; Salvarezza, R. C. Self-Assembled Monolayers of Thiols and Dithiols on Gold: New Challenges for a Well-Known System. *Chem. Soc. Rev.* **2010**, *39*, 1805-1834.
(7) Pensa, E.; Carro, P.; Rubert, A. A.; Benítez, G.; Vericat, C.; Salvarezza, R. C. Thiol with an Unusual Adsorption−Desorption Behavior: 6-Mercaptopurine on Au(111). *Langmuir* **2010**, *26*, 17068-17074.
(8) Jin, Q.; Rodriguez, J. A.; Li, C. Z.; Darici, Y.; Tao, N. J. Self-Assembly of Aromatic Thiols on Au(111). *Surf. Sci* **1999**, *425*, 101-111.
(9) Pensa, E.; Rubert, A. A.; Benitez, G.; Carro, P.; Orive, A. G.; Creus, A. H.; Salvarezza, R. C.; Vericat, C. Are 4-Mercaptobenzoic Acid Self Assembled Monolayers on Au(111) a Suitable System to Test Adatom Models? *J. Phys. Chem. C* **2012**, *116*, 25765-25771.
(10) Parker, W. B. Enzymology of Purine and Pyrimidine Antimetabolites Used in the Treatment of Cancer. *Chem. Soc. Rev.* **2009**, *109*, 2880-2893.
(11) Lobo Maza, F.; Grumelli, D.; Carro, P.; Vericat, C.; Kern, K.; Salvarezza, R. C. The Role of the Crystalline Face in the Ordering of 6-Mercaptopurine Self-Assembled Monolayers on Gold. *Nanoscale* **2016**, *8*, 17231-17240.
(12) Grumelli, D.; Cristina, L. J.; Maza, F. L.; Carro, P.; Ferrón, J.; Kern, K.; Salvarezza, R. C. Thiol Adsorption on the Au(100)-Hex and Au(100)-(1 × 1) Surfaces. *J. Phys. Chem. C* **2015**, *119*, 14248-14254.
(13) Horcas, I.; Fernandez, R.; Gomez-Rodriguez, J. M.; Colchero, J.; Gomez-Herrero, J.; Baro, A. M. Wsxm: A Software for Scanning Probe Microscopy and a Tool for Nanotechnology. *Rev. Sci. Instrum.* **2007**, *78*, 013705-8.
(14) Yeh, J. J.; Lindau, I. Atomic Subshell Photoionization Cross Sections and Asymmetry Parameters: $1 \leqslant Z \leqslant 103$. *Atomic Data and Nuclear Data Tables* **1985**, *32*, 1-155.
(15)Hermann, K.; Van Hove, M. A. Http://Www.Fhi-Berlin.Mpg.De/Khsoftware/Leedpat/Leedpat4_ Leed Pattern Analyzer.
(16) Kresse, G.; Furthmüller, J. Efficiency of Ab-Initio Total Energy Calculations for Metals and Semiconductors Using a Plane-Wave Basis Set. *Comput. Mater. Sci.* **1996**, *6*, 15-50.
(17) Kresse, G.; Hafner, J. Ab Initio. *Phys. Rev. B* **1993**, *48*, 13115-13118.
(18) Dion, M.; Rydberg, H.; Schröder, E.; Langreth, D. C.; Lundqvist, B. I. Van Der Waals Density Functional for General Geometries. *Phys. Rev. Lett.* **2004**, *92*, 246401.
(19) K, K.; Bowler, D., R. ; Michaelides, A. Chemical Accuracy for the Van Der Waals Density Functional. *J. Phys. Condens. Matter* **2010**, *22*, 022201.
(20) Blöchl, P. E. Projector Augmented-Wave Method. *Phys. Rev. B* **1994**, *50*, 17953-17979.
(21) Monkhorst, H. J.; Pack, J. D. Special Points for Brillouin-Zone Integrations. *Phys. Rev. B* **1976**, *13*, 5188-5192.
(22) Reimers, J. R.; Ford, M. J.; Halder, A.; Ulstrup, J.; Hush, N. S. Gold Surfaces and Nanoparticles Are Protected by Au(0)–Thiyl Species and Are Destroyed When Au(I)–Thiolates Form. *Proc. Natl. Acad. Sci.* **2016**, *113*, E1424-E1433.
(23) Pearson, W. B. *In Handbook of Lattice Spacing and Structure of Metals*; Pergamon Press, Inc.: New York, 1958.

(24) Jiang, Y.; Liang, X.; Ren, S.; Chen, C.-L.; Fan, L.-J.; Yang, Y.-W.; Tang , J.-M.; Luh, D.-A. The Growth of Sulfur Adlayers on Au(100). *J. Chem. Phys.* **2015**, *142*, 064708 1-11.
(25) Hölzle, M. H.; Wandlowski, T.; Kolb, D. M. Phase Transition in Uracil Adlayers on Electrochemically Prepared Island-Free Au(100)−(1 × 1). *J. Electroanal. Chem.* **1995**, *394*, 271-275.
(26) Schreiber, F. Structure and Growth of Self-Assembling Monolayers. *Prog. Surf. Sci.* **2000**, *65*, 151-257.
(27) Grumelli, D.; Maza, F. L.; Kern, K.; Salvarezza, R. C.; Carro, P. Surface Structure and Chemistry of Alkanethiols on Au(100)-(1 × 1) Substrates. *J. Phys. Chem. C* **2016**, *120*, 291-296.
(28) Eisuke, I.; Takayuki, A.; Masahiko, H.; Jaegeun, N. Surface Potential Change Depending on Molecular Orientation of Hexadecanethiol Self-Assembled Monolayers on Au(111). *Bull. Korean Chem. Soc.* **2009**, *30*, 1309-1312.
(29) Löfgren, J.; Grönbeck, H.; Moth-Poulsen, K.; Erhart, P. Understanding the Phase Diagram of Self-Assembled Monolayers of Alkanethiolates on Gold. *J. Phys. Chem. C* **2016**, *120*, 12059-12067.
(30) Reyes, E.; Madueño, R.; Blázquez, M.; Pineda, T. Facile Exchange of Ligands on the 6-Mercaptopurine-Monolayer Protected Gold Clusters Surface. *J. Phys. Chem. C* **2010**, *114*, 15955-15962.
(31) Madueño, R.; Sevilla, J. M.; Pineda, T.; Román, A. J.; Blázquez, M. A Voltammetric Study of 6-Mercaptopurine Monolayers on Polycrystalline Gold Electrodes. *J. Electroanal. Chem.* **2001**, *506*, 92-98.
(32) Leung, T. Y. B.; Gerstenberg, M. C.; Lavrich, D. J.; Scoles, G.; Schreiber, F.; Poirier, G. E. 1,6-Hexanedithiol Monolayers on Au(111): A Multitechnique Structural Study. *Langmuir* **2000**, *16*, 549-561.